

Nonequilibrium Magnetization Dynamics of Nickel

J. Hohlfeld, E. M. Matthias

Institut für Experimentalphysik, Freie Universität Berlin, 14195 Berlin, Germany

R. Knorren, K. H. Bennemann

Institut für Theoretische Physik, Freie Universität Berlin, 14195 Berlin, Germany

()

Ultrafast magnetization dynamics of nickel has been studied for different degrees of electronic excitation, using pump-probe second-harmonic generation with 150 fs/800 nm laser pulses of various fluences. Information about the electronic and magnetic response to laser irradiation is obtained from sums and differences of the SHG intensity for opposite magnetization directions. The classical $M(T)$ -curve can be reproduced for delay times larger than the electron thermalization time of about 280 fs, even when electrons and lattice have not reached thermal equilibrium. Further we show that the transient magnetization reaches its minimum 50 fs before electron thermalization is completed.

PACS numbers: 42.65 Ky, 75.40 Gb, 78.47.+p

Ultrafast spin dynamics in ferromagnets is of great interest from both theoretical and experimental points of view. In particular, the short-time dynamics of magnetism in transition metals, with many excited electrons not at equilibrium with the lattice, is a new area of physics. Such studies are important for developing a theory of transient magnetization behavior in the sub-picosecond range. It seems that the only experimental data which can guide theoretical analysis are the ones reported by Beaurepaire et al. [1] on time-resolved demagnetization of Ni induced by femtosecond laser pulses of 620 nm at one specific fluence. The authors utilized the magneto-optical Kerr effect to detect hysteresis loops for different time delays between pump and probe pulses. By comparing the time-dependent remanence with the equilibrium temperature dependence of magnetization, $M(T)$, they derived the time evolution of the spin temperature within the framework of the phenomenological three-temperature model [2]. Clearly, it is of great importance to confirm whether or not $M(T)$ can be used to describe the transient magnetic response to electron excitations in itinerant ferromagnets and whether there is a time delay between electron thermalization and magnetization changes.

In this Letter we present time-resolved data on the transient magnetization measured by pump-probe second-harmonic generation (SHG). The great advantage of this technique is that it allows to simultaneously follow electron-temperature relaxation and transient magnetization, without further need for additional calibration measurements. This is a consequence of the even and odd contributions to the nonlinear susceptibility [3]. The measurements were carried out for a large variety of pump fluences leading to different initial electron temperatures. After equilibration of the electron bath, we find the transient magnetization to be governed by the electron temperature T_e via the classical $M(T)$ -curve [4]. However, we observe a strong deviation of the data

from the magnetization curve in the short-time range $t < 0.3$ ps, where the electron system is in a nonequilibrium state.

When discussing nonequilibrium spin dynamics in ferromagnets, it is worth noting that relaxation times presented here, where nonequilibrium electronic states are excited, are not compatible with the spin-lattice relaxation times, τ_{sl} . The latter denotes the time it takes for the spin system to adjust to a new temperature while equilibrium between electron and lattice temperature is maintained. Hence, the values of $\tau_{sl} = 100 - 80$ ps measured by Vaterlaus et al. for ferromagnetic Gd [2,5] and the limits given for Fe [5,6] and Ni [7] must be considered in a different context.

Experiments were performed at room temperature on polished polycrystalline nickel (purity 99.90 %) in air. The samples were magnetized to saturation with the magnetization direction oriented perpendicular to the plane of incidence. P-polarized 150 fs/800 nm pump and probe pulses with an intensity ratio of 3:1 for the highest pump fluence were used to excite the electrons and probe electron temperature and magnetization by detecting the reflected unpolarized SHG. Angles of incidence were 20° for the pump and 45° for the probe beams. We do not expect any interfering effects from the nickel oxide layer | which is antiferromagnetic | since we only measured relative changes in SHG yield for opposite magnetization directions [8] as a function of delay time between pump and probe pulses.

Typical relaxation curves are shown in Fig.1 for seven selected pump intensities, although more were measured and included in Fig.3. Displayed are sums and differences of SHG signals for opposite magnetization directions $I_{\pm}(t)$, normalized to the SHG yield I_0 for the probe pulse alone:

$$I_{\pm} = I_{\pm}(t) / I_0 = I_{\pm} / I_0 ; \quad (1)$$

where $I_{\pm} = I(2!; +M) - I(2!; -M)$. The second-order polarization in the presence of magnetization can be written in the form [3]

$$P_i(2!) = \sum_{j,k} \chi_{ijk}^{(2)}(M) E_j E_k + \sum_{j,k} \chi_{ijk}^{(2)}(M) E_j E_k : \quad (2)$$

The even tensor elements are almost unaffected by the magnetization, whereas the odd ones scale linearly with M [9]. Hence, we can substitute:

$$\chi_{ijk}^{(2)}(M) = \chi_{ijk}^{(2)} + \chi_{ijk}^{(2)}(M) ; \quad \chi_{ijk}^{(2)}(M) = \chi_{ijk}^{(2)} + \chi_{ijk}^{(2)}(M) : \quad (3)$$

From Eq.2 we obtain the expressions

$$I_{\pm} = 2 \sum_{j,k} \chi_{ijk}^{(2)}(M) E_j E_k + \sum_{j,k} \chi_{ijk}^{(2)}(M) E_j E_k ; \quad (4)$$

$$I = 4 \sum_{j,k} \chi_{ijk}^{(2)}(M) E_j E_k \cos \theta ; \quad (5)$$

where the individual tensor elements are combined to an effective even and odd contribution denoted by $\chi_{0j}^{(2)}$

and χ_0^{odd} . A and B represent the corresponding effective Fresnel coefficients for the fundamental and frequency-doubled light [10]. The resulting phase of A , B , χ_0^{even} , and χ_0^{odd} depends on M and is given by ϕ . Measurements of transient linear reflectivities (not shown here) verify that the magnitude of the Fresnel factors A and B is nearly unaffected by T_e . Also, calculations reveal that the magnetization-independent factors χ_0^{even} and χ_0^{odd} vary only a few percent with T_e for $T_e > T_C$ (T_C = Curie temperature). This can be understood by the large width (~ 0.3 eV) of vacant d-states in the minority band [11] in comparison with the maximum electron temperature of 550 K reached with the highest pump fluence. Thus, we conclude that the time dependence of I is contained in $M(t)$. Assuming $M(t) = M(T_e(t))$, the classical $M(T)$ -curve [4] can be approximated by $M(T_e) = M(T_0) [\text{const} \cdot (T_e - T_0)]^{1/2}$ for the electron-temperature range covered in our experiment. Here, T_0 denotes the mean electron temperature at negative delay. Inserting this into Eqs. (1), (4), and (5) we obtain

$$I^+(t) = \text{const} \cdot [B - T_e(t)] ; \quad (6)$$

$$I^-(t) = \frac{M(T_e(t)) \cos \phi}{M(T_0)} - 1 ; \quad (7)$$

Prerequisite for the validity of these equations is a thermalized electron distribution. Thus for $t > 0.3$ ps the curves in Fig. 1a represent the time evolution of electron temperature, while those in Fig. 1b describe the transient magnetization, provided ϕ is constant. That I^+ is indeed proportional to temperature can be verified by plotting the averaged values for delay times > 3 ps in Fig. 1a against fluence. The result is shown in Fig. 2. In thermal equilibrium with the lattice, T_e scales linearly with fluence. The slope $m = 1$ in Fig. 2 proves this proportionality in Eq. 6 and hence the validity of our approximation for $M(T_e)$ for longer delay times.

Eqs. 6 and 7 suggest a graph of $(I^- + 1)$ versus I^+ which can be compared with the classical $M(T)$ -curve for nickel [4]. Such plot is shown in Fig. 3. In the upper frame [Fig. 3a], only data for delay times > 0.3 ps have been analyzed. Obviously, this plot reproduces within 5% the equilibrium magnetization curve, indicated by the solid line. The good agreement justifies the above made assumptions and demonstrates that ϕ does not depend significantly on $T_e(t)$. Furthermore, it provides an intrinsic electron-temperature calibration for excitation with various pump intensities. It must be emphasized that this agreement includes the range between 0.3 ps and 3 ps where T_e is not in equilibrium with the lattice temperature [cf. Fig. 1]. We also conclude from Fig. 3a that the electron temperature governs magnetization. From the delay time where the points fall on the magnetization curve we can unambiguously conclude that the electrons are fully thermalized after ~ 280 fs, when the minima in Fig. 1a are reached.

The nonequilibrium situation is demonstrated by incorporating the data for $t < 0.3$ ps into the same plot, as illustrated in Fig.3b for three fluences. The strong deviation of the data from the magnetization curve can be attributed to nonequilibrium electrons, and, in view of Eq. (5), to a rapid phase change. It vanishes when the thermalization of the electron gas is completed, and then the data again follow the magnetization curve.

The different behavior of nonequilibrium electrons becomes more evident in the real-time plot of I^+ and I^- in Fig.4, which is a magnified version of the short-time range in Fig.1. For clarity, only data for three fluences are displayed, but the same delay between the minima of I^+ and I^- is observed for all fluences. The minima of I^+ at (280 ± 30) fs (dotted line in Fig.4a) mark the time at which the thermalization of the electrons is completed and agrees with the value reported by Beaurepaire et al. [1]. The breakdown of I^- in Fig.4b follows the convolution of pump and probe pulses. For all fluences the minimum is reached about 50 fs before the electron temperature is established. To understand the faster response of I^-/M compared to I^+ we notice that for $t < 0.3$ ps Eq. (6) is no longer valid and $I^+ \propto M^2$. This means that I^+ reflects the momentary population difference between minority and majority spins and, therefore, monitors the development of electron temperature out of a highly nonequilibrium state [12]. I^- is in addition sensitive to the direction of M and samples preferentially the minority spins of the vacant d-states. Note, that the spin-orbit coupling is restored faster for minority than for majority spins [13], since the width of the vacant d-states (~ 0.3 eV) is large compared to the Fermi distribution for $T_e \sim T_c$. The shift in Fig.4 and the fact the magnetization curve is reproduced after thermalization of the electrons prove that for $t \sim 280$ fs the electron temperature governs the magnetization. This is in striking contrast to the results reported by Beaurepaire et al. [1] who observed a 2 ps delayed magnetic response with respect to T_e . Further investigations are required to elucidate the cause of these deviating observations, since too many parameters differ in the experiments reported here and in [1]. Note, however, that the response time of itinerant magnetism is expected to be of the order of T_c^{-1} , corresponding to about 80 fs for Ni.

Let us return to Fig.1 and attempt to understand the large decrease of I^- in terms of the band structure. The fundamental wavelength of 800 nm (1.55 eV) matches well the difference between the two main peaks of the Ni minority band [11], as sketched in Fig.5. Due to the exchange splitting, the upper peak is unoccupied for minority spins and can resonantly enhance the SHG in the intermediate state. For majority spins there is no such enhancement. The filling of the vacant states in the minority d-band causing the breakdown of M reduces this resonance enhancement which leads to the fluence-dependent drop of signals in Fig.1. The effect is further

amplified by the large matrix elements for d-d transitions [14]. The size of reduction of I^+ is determined by the ratio of odd to even parts of the nonlinear susceptibility and the corresponding Fresnel factors. Using the temperature calibration via Figs. 2 and 3, one can derive from Eqs. (3) and (4) the ratio $\beta_0^{\text{odd}}/\beta_0^{\text{even}} = 0.7 \pm 0.1$.

Summarizing, we have shown that pump-probe SHG is a powerful method for investigating ultrafast spin dynamics in ferromagnets, since it contains information about both, electron temperature and magnetization. We applied different pump fluences to study the electron and spin dynamics for various degrees of excitation. Independently of pump fluence, the electron thermalization is completed after (280 ± 30) fs and the magnetization curve [4] is reproduced from this time on, even when the electrons are not in equilibrium with the lattice. For the first time we have observed that the magnetic response is faster than the electron thermalization, which may be attributed to different lifetimes of excited majority and minority electrons. Further investigations of this topic, in particular frequency-dependent measurements which may uncover band-structure effects, are desirable.

This work was supported by the Deutsche Forschungsgemeinschaft, Sfb 290.

-
- [1] E. Beaurepaire, J.C. Merle, A. Daunois, J.-Y. Bigot, Phys. Rev. Lett. 76, 4250 (1996) and references therein
 - [2] A. Vaterlaus, T. Beutler, F. Meier, Phys. Rev. Lett. 67, 3314 (1991)
 - [3] R.P. Pan, H.D. Wei, Y.R. Shen, Phys. Rev. B 39, 1229 (1989)
 - [4] P. Weiss and R. Forrer, Ann. Phys. 5, 153 (1926)
 - [5] A. Vaterlaus et al., Phys. Rev. B 46, 5280 (1992)
 - [6] A. Vaterlaus et al., J. Appl. Phys. 67, 5661 (1990)
 - [7] M.B. Agranat et al., Zh. Eksp. Teor. Fiz. 86, 1376 (1984) [Sov. Phys. JETP 59, 804 (1984)]
 - [8] K. Bohmer, J. Hohlfeld, E. M. Atthias, Appl. Phys. A 60, 203 (1995)
 - [9] U. Pustogowa, W. Hubner, K.H. Bennemann, Surf. Sci. 307-309, 1129 (1994)
 - [10] J.E. Sipe, D.J. Moss, H.M. van Driel, Phys. Rev. B 35, 1129 (1987)
 - [11] J. Callaway, C.S. Wang, Phys. Rev. B 7, 1096 (1973)
 - [12] W.S. Fann et al., Phys. Rev. B 46, 13592 (1992)
 - [13] D.R. Penn, S.P. Apell, S.M. Girvin, Phys. Rev. B 32, 7753 (1985)
 - [14] W. Hubner, K.H. Bennemann, K. Bohmer, Phys. Rev. B 50, 17597 (1994)

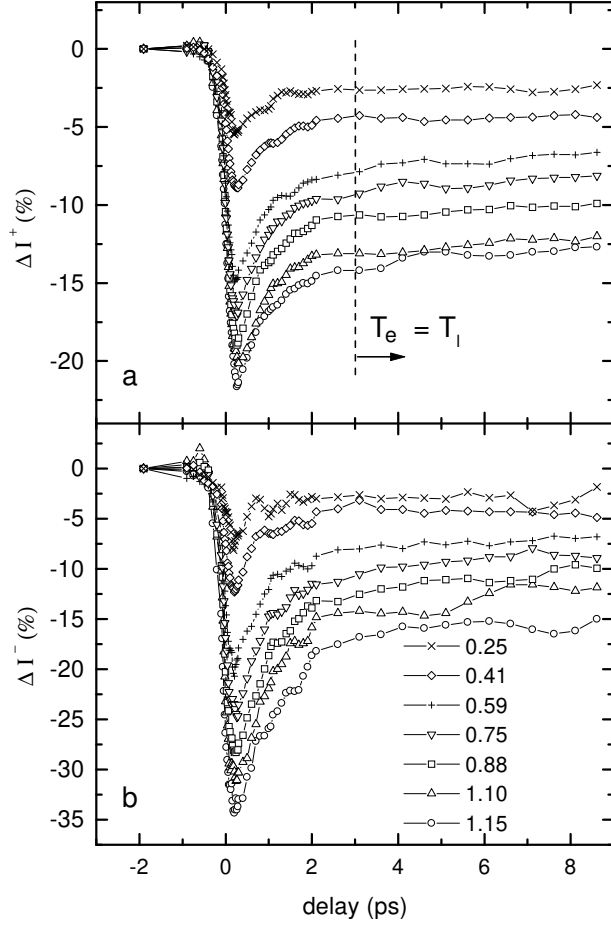


FIG. 1. Time dependence of normalized sums (a) and differences (b) of SHG yields for opposite magnetization directions, as defined in Eq. (1). The curves were recorded with different relative fluences, calibrated by $1.00 \pm 0.06 \text{ mJ/cm}^2$. Constant levels for $t > 3 \text{ ps}$ reflect equilibrium between electron and lattice temperatures, T_e and T_l .

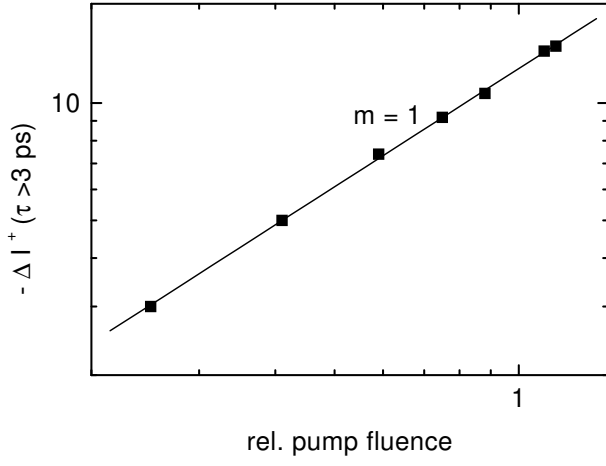


FIG. 2. Normalized sums of SHG yields for opposite magnetization directions, averaged over all values for $t > 3$ ps, as a function of relative fluence. The linear slope indicates that I^+ is proportional to electron temperature [see Eq. (6)].

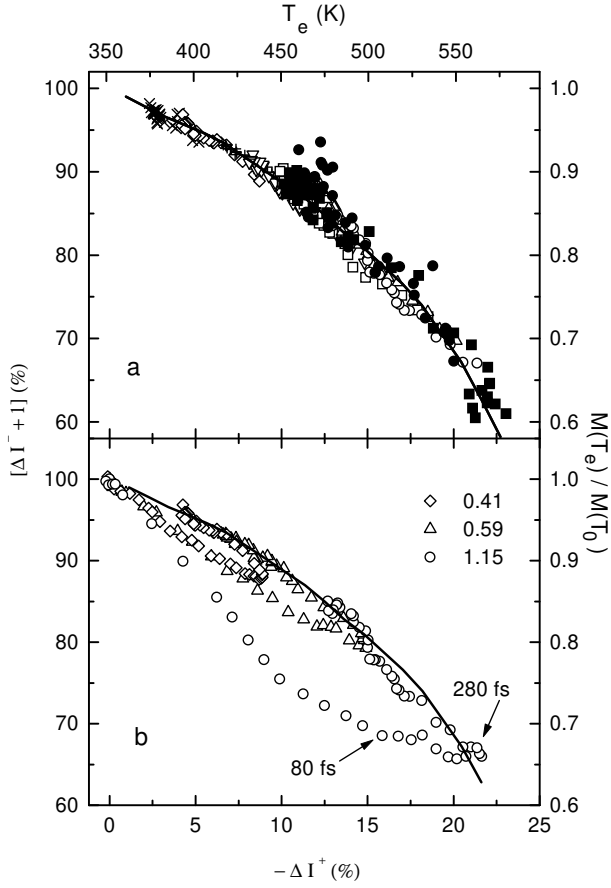


FIG. 3. (a) Comparison of all measured data for $t > 0.3$ ps with the equilibrium magnetization curve of Ref. [4], represented by the solid line. (b) Data for three selected fluences covering the total time range. Deviations from the magnetization curve point to a nonequilibrium state of the electron and spin systems for $t < 0.3$ ps.

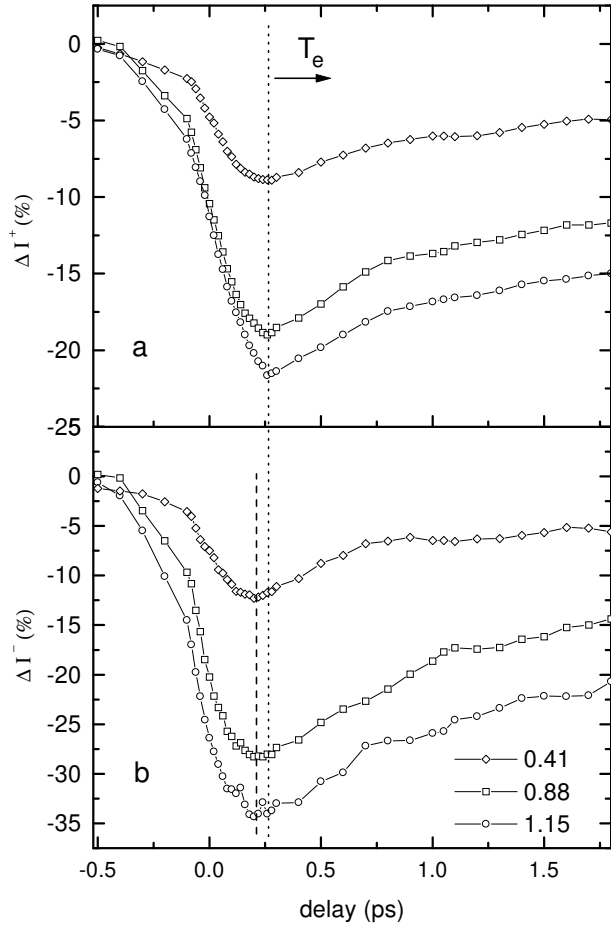


FIG. 4. Magnified version of Fig. 1 for three selected fluences. The minima at (280 ± 30) fs in (a), marked by the dotted line, signal the onset of a well defined electron temperature. The minima in (b) occur 50 fs faster (dashed line).

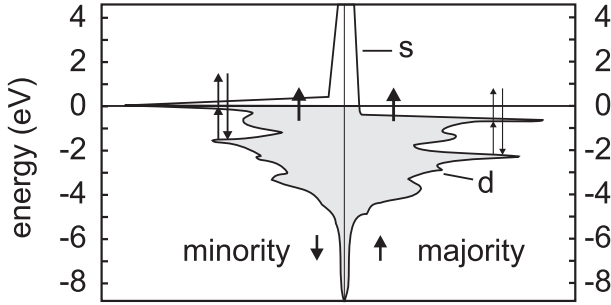


FIG. 5. Density of states for minority and majority spins according to Callaway and Wang [11]. While single-photon excitation proceeds with comparable rates from both parts, SHG is resonantly enhanced by the unoccupied peak in the minority band.